PRAMANA
— journal of
physics

Vol. 61, No. 3
September 2003
pp. 507–515

Hexadecapole deformation studies in ^{148,150}Nd

B S NARA SINGH, V NANAL and R G PILLAY
Tata Institute of Fundamental Research, Homi Bhabha Road, Mumbai 400 005, India
Email: pillai@tifr.res.in

MS received 5 July 2002; revised 18 January 2003; accepted 21 February 2003

Abstract. The γ-ray yields from inelastically excited 2^+ and 4^+ levels of ^{144,146,148,150}Nd nuclei using ^{16}O beam at near barrier energies in coincidence with the back-scattered projectiles were measured. The 2^+ and 4^+ level cross-sections were deduced from the measured γ-ray yields and fitted to the DWBA calculations to obtain the reduced transition matrix elements $M(E4 : 0^+ \rightarrow 4^+)$. The deduced $M(E4)$ values for ^{148}Nd and ^{150}Nd nuclei, 0.16(0.05) and 0.22(0.12) eb^2, respectively are consistent with theoretical predictions.

Keywords. Deformation; hexadecapole moments; Coulomb excitation.

PACS Nos 21.10.Ky; 27.70.+q; 25.70.De

1. Introduction

It is well-known that the static deformations play an important role in understanding various nuclear phenomena. Both ground state and dynamical properties of nuclei are deformation dependent [1] and hence the measurements of deformation parameters furnish good testing grounds for nuclear structure models. The stability of nuclei in the superheavy mass regions as well as near proton and neutron driplines critically depends on deformations. Although in general the quadrupole deformation (β_2) is sufficient to explain most of the nuclear phenomena, in the rare-earth and the actinide regions hexadecapole deformation (β_4) becomes important [2,3]. For example, the interacting boson model (IBM) [4] with only monopole and quadrupole degrees of freedom (sd-IBM) predicts a larger effective charge for neutrons compared to that of protons in the rare-earth region which is physically incorrect. This inconsistency was resolved by the inclusion of hexadecapole degree of freedom (viz. g-boson) [5].

The hexadecapole nuclear deformations were first accurately measured by scattering of α particles at energies well above the Coulomb barrier for rare-earth nuclei [6]. Since then, systematic trends in deformations (β_2, β_4, β_6) have been established in rare-earth nuclei [7,8] and also in actinide region [9–11] using experimental techniques like Coulomb excitation (Coulex) [12] and Coulomb nuclear interference (CNI) [13]. A compilation of measured β_4 values in rare-earth region together with predictions from model calculations

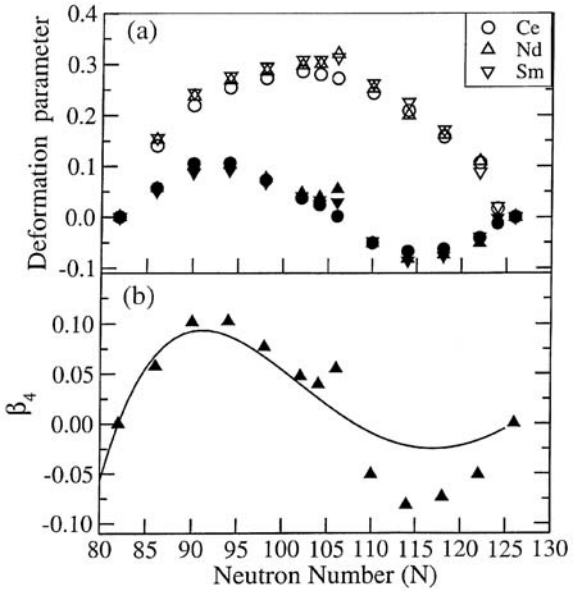

Figure 1. (**a**) The deformation parameters β_2 (open symbols) and β_4 (filled symbols) as a function of neutron number obtained from potential energy minimizing calculations using a Woods–Saxon potential for $Z = 58$, 60 and 62; (**b**) a comparison of β_4 for Nd (filled triangles) in (a) with the semi-empirical model calculations (solid line) (see text for details).

is given in ref. [3]. The trends in β_4 are found to be in general agreement with the theoretical predictions.

Figure 1a shows our predictions on β_2 and β_4 for Ce, Nd and Sm nuclei as a function of neutron number from the potential energy minimization calculations using a Woods–Saxon form for the nuclear potential instead of the modified harmonic oscillator potential used in the calculations described in ref. [14]. The β_2 values peak at mid-shell as expected, while the β_4 values peak at 1/4th and 3/4th of shell filling. These calculations are compared with a semi-empirical model [15] in figure 1b. It should be noted that for the stable Nd isotopes, namely, ^{142}Nd ($N = 82$, spherical) to ^{150}Nd ($N = 90$, strongly deformed), β_4 value increases from 0 to 0.102 (corresponding $M(E4 : 0^+ \rightarrow 4^+) \sim 0$ to 0.25 eb^2). Also, in the $SU(3)$ limit of sdg-IBM for axially symmetric deformed nuclei, $M(E4)$ increases linearly with the number of bosons [16]. The sdg-IBM predicts for ^{142}Nd to ^{150}Nd a rapid increase in $M(E4)$ from 0 to 0.26 eb^2 (corresponding $\beta_4 \sim 0$ to 0.105) consistent with our calculations. However, the available data [17] (although the uncertainties are large) shows a decrement in $M(E4)$ from ^{148}Nd (0.30$\pm$0.11 eb^2) to ^{150}Nd (0.25$\pm$0.12 eb^2).

To measure the β_4 values with better accuracies and resolve these discrepancies, we propose a new experimental technique using heavy ion projectiles at energies close to and below the Coulomb barrier [18]. In the present technique, the inelastic cross-sections are obtained by measuring the de-exciting γ-rays in coincidence with the scattered projectiles. Since heavy ions have larger cross-sections and the detection of γ-rays enables the usage of thick targets ($\sim$1 mg/cm^2), this technique is expected to yield a better statistical accuracy

in comparison with Coulex and CNI methods. At near barrier energies only the exponential tail of nuclear potential plays a role and hence the inelastic cross-sections are not very sensitive to variations in optical model parameters. Further, the simultaneous measurement of 2^+ and 4^+ level cross-sections together with elastic scattering cross-section can be used to constrain the nuclear potential. The present technique attempts to combine the advantages of Coulex and CNI, while trying to overcome the uncertainties arising due to the nuclear potential.

We carried out β_4 measurements for the strongly deformed ^{148,150}Nd using the technique described above. The γ-ray yields from inelastically excited 2^+ and 4^+ levels of ^{144,146,148,150}Nd nuclei in coincidence with the back-scattered ^{16}O projectiles were measured. The 2^+ and 4^+ level cross-sections were deduced from the measured γ-ray yields and fitted to the DWBA calculations to obtain the reduced transition matrix elements $M(E4)$.

2. Experimental details

The experiments were carried out with the TIFR-BARC 14UD Pelletron in Mumbai, India. The well-collimated ^{16}O beams of energy $E_{\rm inc} = 54$–67 MeV with typical beam currents in the range of 10–15 nA were used. The targets, with $\sim$1 mg/cm^2 thickness, were prepared by rolling natural neodymium metal typically 10 h before the experiment and stored in a vacuum desiccator to avoid deterioration by exposure to air. The gold-backed Nd targets were prepared by rolling the 1 mg/cm^2 $^{\rm nat}$Nd foil onto a 4 mg/cm^2 Au foil. Self-supporting targets were used to measure the γ-ray yields from the excited states of different Nd isotopes having short half-lives, while for those states having large lifetimes (namely, 2^+ level of ^{150}Nd with $T_{1/2} = 1.49$ ns) the backed targets were used. The use of natural Nd target permitted simultaneous measurement of the inelastic scattering from all stable Nd isotopes.

The experimental setup is schematically shown in figure 2. The γ-rays were detected in three efficiency calibrated HPGe Clover detectors, each consisting of four individual elements, kept at a distance of 10 cm from the target. The individual elements of the Clover detectors 2 and 3 were at mean angles of 32°, 58° while those of Clover 1 were at 122° and 148° with respect to the beam direction. An annular Si surface barrier detector, kept at 4 cm distance from the target, detected the back-scattered projectiles at a mean lab angle of 173°. The geometry of the particle detector was verified by measuring the Rutherford scattering cross-section from a thin gold target ($\sim$200 μg/cm^2). The average thickness of Nd target was also obtained from the Rutherford back-scattered spectra. Quasi-elastic scattering of ^{16}O from a thin enriched ^{150}Nd target ($\sim$15 μg/cm^2) in the range $\theta_{\rm lab} = 86$–$168°$ and $E_{\rm inc} = 54$–70 MeV was measured in a separate experiment. These data were used to fix the optical potential for ^{16}O + $^{\rm nat}$Nd system.

The de-exciting γ-rays from the inelastically excited 2^+ and 4^+ states of the Nd isotopes were detected in coincidence with the scattered projectiles in the annular detector. For every event, the data consisting of γ-ray energies, particle energies and particle-γ time were recorded in listmode. The data reduction and analysis were done using programs developed by us and the package FREEDOM [19].

Table 1 lists the different γ-ray lines of interest in Nd isotopes. As mentioned earlier, the backed target data was used in extracting the yield for 130 keV transition. It was necessary to use self-supporting target for other lines of interest where lifetimes are comparable to

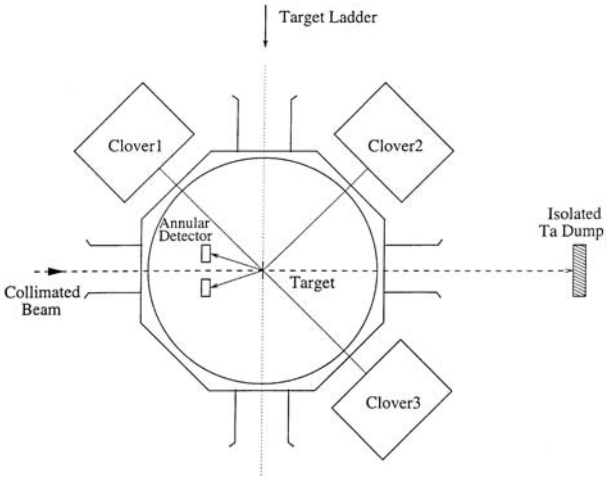

Figure 2. A schematic picture of the experimental setup used for β_4 measurements.

Table 1. Nd isotope data.

Isotope (abundance)	Transition	E_γ (keV)	$T_{1/2}$
^{144}Nd (23.80%)	$2^+ \rightarrow 0^+$	696	3.40 ps
^{146}Nd (17.20%)	$2^+ \rightarrow 0^+$	454	21.60 ps
^{148}Nd (5.76%)	$2^+ \rightarrow 0^+$	301	78.00 ps
	$4^+ \rightarrow 0^+$	450	7.03 ps
^{150}Nd (5.64%)	$2^+ \rightarrow 0^+$	130	1.49 ns
	$4^+ \rightarrow 0^+$	250	63.00 ps

stopping time. Also for 450 keV (^{148}Nd) and 454 keV (^{146}Nd) γ-rays, only data at 122° and 148° were used. These lines were not very well resolved in forward detectors because of the lineshape of 450 keV line. Typical coincidence spectra, namely, chance corrected γ-ray spectrum, particle energy spectrum and particle-γ time spectrum for 64 MeV ^{16}O beam on a self-supporting Nd target are shown in figure 3. Various γ-rays corresponding to the de-excitation of 2^+ and 4^+ levels of Nd isotopes are clearly identified. At energies close to the Coulomb barrier, in addition to inelastic excitation, other surface reactions like α-transfer channel become visible and can be seen as a small peak to the left of the quasi-elastic peak in the particle spectra. Low energy light charged particles resulting from reactions of beam halo hitting the collimator of annular detector can also be seen. The tail on the right side of the particle-γ time prompt is due to the walk in the CFD for low energy γ-rays. Hence, the chance correction for 130 keV and 250 keV γ-rays had to be done taking into account the relatively wider prompt windows. In obtaining the cross-sections, the γ-ray yields were corrected for the detector efficiency, internal conversions and particle-γ angular correlations. The Clover detector efficiency was measured with calibrated ^{152}Eu

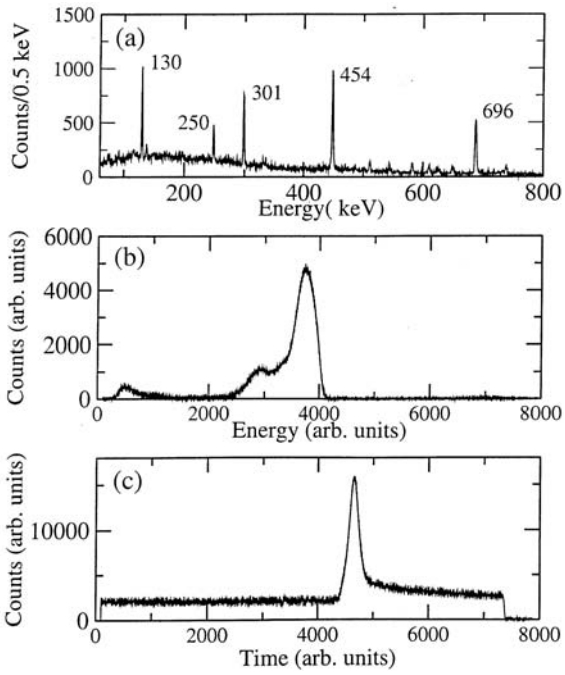

Figure 3. Coincidence spectra for 64 MeV ^{16}O beam on a self-supporting 1 mg/cm^2 thick ^{nat}Nd target. (**a**) A typical γ-ray spectrum, (**b**) back-scattered particle energy spectrum in the annular detector and (**c**) particle-γ time spectrum.

and ^{133}Ba sources at the target position. The internal conversion coefficients are taken from the tables given in ref. [20]. The correction was also done to take into account the feeding from 4^+ level in obtaining the 2^+ cross-section for deformed Nd isotopes. The feeding from 6^+ level to 4^+ level is insignificant under the present experimental conditions and hence neglected.

The back-scattered projectiles predominantly populate $m = 0$ substate ($\geq$99%). Therefore the particle-γ angular correlations were calculated for θ_γ corresponding to each Clover element, namely, 32°, 58°, 122° and 148°, using the theoretical values for angular distribution coefficients of $m = 0$ target substates and the feeding coefficients (U-factors) [21]. These calculated values were averaged over all four elements of each Clover detector and the derived mean values, namely, 1.48(0.06) for $2^+ \rightarrow 0^+$ and 1.19(0.05) for $4^+ \rightarrow 2^+$ were used in the present analysis. Attenuations of these coefficients due to de-orientation of target m-substates were estimated to be negligible when Au-backed targets were used [22].

3. Results and discussion

In order to get $d\sigma(2^+)/d\Omega$ and $d\sigma(4^+)/d\Omega$ from the measured γ-ray yields, the target thickness and the number of incident particles is required. In the present experiment, to achieve high particle-γ coincidence efficiency, thick Nd targets were used in conjunction

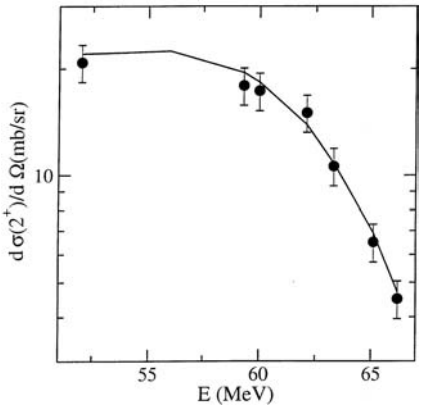

Figure 4. The inelastic cross-section $d\sigma(2^+)/d\Omega$ for ^{146}Nd deduced from the measured γ-ray yield (as described in the text) together with ECIS calculations (solid line) using the optical potential deduced from ^{144}Nd but with $W_{s0} = -7$ MeV (see text for details).

with a compact chamber geometry. As a result of this, the charge integration used to measure the number of incident beam particles was found to be unreliable. Moreover, the rolled thick Nd targets were highly non-uniform resulting in uncertainties in the target thickness. We therefore derived the normalization constants by fitting the γ-ray yield data for near spherical ^{144,146}Nd nuclei. From the available data for $d\sigma(0^+)/d\Omega$ and $d\sigma(2^+)/d\Omega$ of ^{144,146}Nd at $E_{lab} = 65.1$ MeV in the range $\theta_{cm} = 120$–150° [23], an optical potential was deduced. This otential was used to compute $d\sigma(2^+)/d\Omega$ for ^{144}Nd over the energy range of the present experiment, $E_{lab} = 52$–66.2 MeV, using both ECIS [24] and CSC [25,26] codes. The normalization constants at each incident energy were obtained by comparing the measured γ-ray yields of $2^+ \rightarrow 0^+$ transitions with the computed cross-sections $d\sigma(2^+)/d\Omega$. This normalization procedure was then cross-checked with ^{146}Nd data. A good agreement between theoretical calculations and data can be seen from figure 4. The experimentally deduced $d\sigma(2^+)/d\Omega$ and $d\sigma(4^+)/d\Omega$ are plotted as a function of energy for ^{148}Nd (left panels) and ^{150}Nd (right panels) in figure 5. Errors on data points include statistical as well as systematic errors due to normalization.

The nuclear potential comprises of real and imaginary parts and can be given by $V_N(r) = V(r) + iW(r)$. The absorptive potential can be written as $W(r) = W_v(r) + W_s(r)$, where $W_v(r)$ and $W_s(r)$ are volume and surface contributions, respectively [27]. Both $V(r)$ and $W_v(r)$ have Woods–Saxon forms given by

$$V(r) = \frac{V_0}{1+\exp\left(\frac{r-R_0}{a_0}\right)}, \quad W_v(r) = \frac{W_{v0}}{1+\exp\left(\frac{r-R_w}{a_w}\right)}$$
$$R_0 = r_0(A_p^{1/3} + A_t^{1/3}), \quad R_w = r_w(A_p^{1/3} + A_t^{1/3}), \tag{1}$$

where A_p and A_t are the projectile and target masses, respectively. The surface potential $W_s(r)$ is taken as a derivative of Woods–Saxon form given by

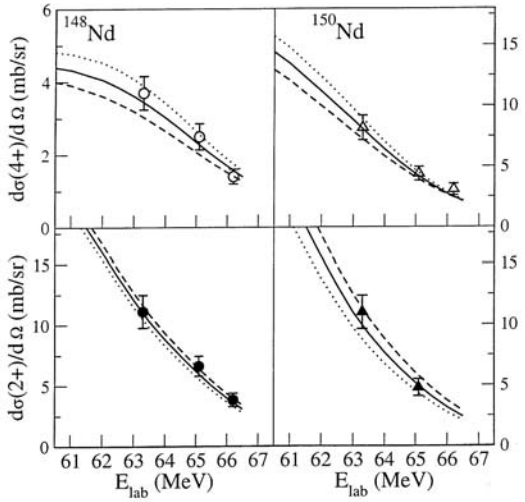

Figure 5. The $d\sigma(4^+)/d\Omega$ and $d\sigma(2^+)/d\Omega$ for ^{148}Nd (circles) and for ^{150}Nd (triangles) plotted as a function of $E_{\rm lab}$. Solid lines correspond to β_4 for the best fit while dashed and dotted lines correspond to lower and upper β_4 limits, respectively. Errors on data points include statistical as well as systematic errors due to normalization.

$$W_{\rm s}(r) = 4\frac{\rm d}{{\rm d}R_{\rm s}}\left(\frac{W_{\rm s0}}{1+\exp(\frac{r-R_{\rm s}}{a_{\rm s}})}\right). \tag{2}$$

It should be pointed out that the volume imaginary potential $W_{\rm v}(r)$ represents fusion. It varies smoothly with the size of the nucleus and the fusion radius r_w is usually smaller than mass radius r_0. The surface imaginary potential $W_{\rm s}(r)$ represents the inelastic channels (due to the surface interactions) and depends on the mass as well as on the shape of a nucleus. The optical model parameters deduced from ^{144}Nd as explained above are:

$$\begin{aligned} &V_0 = -48 \text{ MeV}, \quad W_{\rm v0} = -15 \text{ MeV}, \quad W_{\rm s0} = -5 \text{ MeV}, \\ &r_0 = 1.197 \text{ fm}, \quad r_w = 1.000 \text{ fm}, \quad r_{\rm s} = 1.197 \text{ fm}, \\ &a_0 = 0.600 \text{ fm}, \quad a_w = 0.600 \text{ fm}, \quad a_{\rm s} = 0.700 \text{ fm}. \end{aligned}$$

These are essentially same as Akyüz and Winther parametrization [28] except for the depth of the real potential ($V_0^{\rm AW} = -57$ MeV). The experimental data could also be reproduced for V_0 in the range of -40 to -57 MeV implying that the cross-sections are not strongly sensitive to the optical model parameters. It was necessary to vary $W_{\rm s0}$ as mentioned above for Nd isotopes, namely, $A = 144$ (spherical) to 150 (deformed). We have used $W_{\rm s0} = -7, -10$ and -11 MeV for $A = 146$, 148 and 150, respectively. This choice of $W_{\rm s0}$ also fits the present quasi-elastic scattering data for ^{16}O + ^{150}Nd system.

The inelastic cross-sections are strongly sensitive to β_4 around the Coulomb barrier (59.6 MeV in the center-of-mass). Thus the data at $E_{\rm lab} = 63.3$, 65.1 and 66.2 MeV were used to obtain the β_4 values. Figure 5 shows the calculated $d\sigma(2^+)/d\Omega$ and $d\sigma(4^+)/d\Omega$ as a function of energy corresponding to β_4 values of 0.07(0.02) for ^{148}Nd and 0.09(0.05) for ^{150}Nd. The solid lines in the figure correspond to mean β_4 values while dashed and dotted

lines represent lower and upper β_4 limits respectively. The corresponding reduced transition matrix elements, $M(E4: 0^+ \rightarrow 4^+)$, 0.16(0.05) for ^{148}Nd and 0.22(0.12) eb^2 for ^{150}Nd are consistent with the predicted theoretical trend from sdg-IBM and from our calculations with Woods–Saxon potential.

4. Conclusions

The γ-ray yields from inelastically excited ^{144,146,148,150}Nd nuclei by ^{16}O projectiles in the energy range $E_{\rm inc} = 54$–67 MeV were measured. The optical potential was fixed from the available data of ^{144}Nd and imaginary surface potential W_{s0} was varied as a function of mass. From the deduced $d\sigma(2^+)/d\Omega$ and $d\sigma(4^+)/d\Omega$ of ^{148,150}Nd nuclei, the hexadecapole moments were obtained. The β_4 values 0.07(0.02) and 0.09(0.05) for ^{148}Nd and ^{150}Nd, respectively are in agreement with the predicted values (0.081 and 0.102) from the calculations done with Woods–Saxon potential.

The inelastic cross-section for the 4^+ level is strongly sensitive to β_4 due to the nuclear contributions at energies near the Coulomb barrier. At these energies only the exponential tail of the nuclear potential plays a role and hence the 2^+ and 4^+ level cross-sections are not critically dependent on the choice of the optical model parameters. Further, the present method can be extended to obtain *m*-substate populations ($m \neq 0$) by measuring the γ-ray and particle angular distributions. The *m*-substate populations are strongly sensitive to the Coulomb-nuclear interference effects and thus uncertainties in the extracted β_4 values can be further reduced. Wherever possible, usage of enriched targets would lead to cleaner extraction of cross-sections. As a whole, this method could be used to update data on β_4 values.

Acknowledgements

We are grateful to Prof. C V K Baba for his valuable suggestions and support during the analysis. We thank Dr A Navin for his support during the experiment and Dr J A Sheikh for his assistance in the potential energy minimization calculations. We also thank S Lakshmi, Umesh Kadhane, S M Davane and the Pelletron accelerator staff for their help during the experiment; H Mazumdar and B Behera for providing the enriched ^{150}Nd target.

References

[1] B R Mottelson and S G Nilsson, *Mat. Fys. Skr. Dan. Vid. Selsk* **1**, 8 (1959)
[2] D L Hendrie, *Phys. Rev. Lett.* **31**, 478 (1973)
[3] Y D Devi and V K B Kota, *Pramana – J. Phys.* **39**, 413 (1992) and references therein
[4] F Iachello and A Arima, *The interacting boson model* (University Press, Cambridge, 1987)
[5] O Scholten, R M Ronningen, A Ahmed, G Bomar, H Crowell, J H Hamilton, H Kawakami, C F Maguire, W G Nettles, R B Piercey, A V Ramayya, R Soundranayagam and P H Stelson, *Phys. Rev.* **C34**, 1962 (1986)
[6] D L Hendrie, N K Glendenning, B G Harvey, O N Jarvis, H H Duhm, J Saudinos and J Mahoney, *Phys. Lett.* **B26**, 127 (1968)

[7] R M Ronningen, J H Hamilton, L Varnell, J Lange, A V Ramayya, G Garcia-Bermudez, W Lourens, L L Riedinger, F K McGowan, P H Stelson, R L Robinson and J L C Ford Jr., *Phys. Rev.* **C16**, 2208 (1977)
[8] I Y Lee, J X Saladin, J Holden, J O'Brien, C Baktash, C Bemis Jr., P H Stelson, F K McGowan, W T Milner, J L C Ford Jr., R L Robinson and W Tuttle, *Phys. Rev.* **C12**, 1483 (1975)
[9] J L C Ford Jr., P H Stelson, C E Bemis Jr., F K McGowan, R L Robinson and W T Milner, *Phys. Rev. Lett.* **27**, 1232 (1971)
[10] D L Hendrie, B G Harvey, J R Meriwether, J Mahoney, J C Faivre and D G Kovar, *Phys. Rev. Lett.* **30**, 571 (1973)
[11] F K McGowan, C E Bemis Jr., J L C Ford Jr., W T Milner, R L Robinson and P H Stelson, *Phys. Rev. Lett.* **27**, 1741 (1971)
[12] F S Stephens, R M Diamond and J de Boer, *Phys. Rev. Lett.* **27**, 1151 (1971)
[13] W Bruckner, J G Merdinger, D Pelte, U Smilansky and K Traxel, *Phys. Rev. Lett.* **30**, 57 (1973)
[14] S G Nilsson, C F Tsang, A Sobiczewski, Z Szymanski, S Wycech, C Gustafson, I L Lamm, P Moller and B Nilsson, *Nucl. Phys.* **A131**, 1 (1969)
[15] J Janecke, *Phys. Lett.* **B103**, 1 (1981)
[16] A Arima and F Iachello, *Ann. Phys.* **99**, 253 (1976)
[17] A Ahmed, G Bomar, H Crowell, J H Hamilton, H Kawakami, C F Maguire, W G Nettles, R B Piercey, A V Ramayya, R Soundranayagam, R M Ronningen, O Scholten and P H Stelson, *Phys. Rev.* **C37**, 1836 (1988)
[18] B S Nara Singh, V Nanal and R G Pillay, in *Nuclear structure and dynamics* edited by A K Jain and R K Bhowmik (Phoenix Publishing House Pvt Ltd, New Delhi, 2000) p. 108
[19] B P Ajit Kumar, E T Subrahmanian, R K Bhowmik and K M Jayan, Internal Report (Nuclear Science Centre, New Delhi, India) (unpublished)
[20] K Siegbahn, *Beta- and gamma-ray spectroscopy* (North-Holland Publishing Company, 1955)
[21] H Morinaga and T Yamazaki, *In-beam gamma-ray spectroscopy* (North-Holland Publishing Company, 1976)
[22] I Ben-Zvi, P Gilad, M Goldberg, G Goldring, A Schwarzschild, A Springzak and Z Vager, *Nucl. Phys.* **A121**, 592 (1968)
[23] S K Mandal, *Investigation of quasi-elastic scattering around the barrier in a complex microscopic potential formalism*, Ph.D. thesis (University of Kalyani, Kalyani, India, 1997)
[24] J Raynal, *Phys. Rev.* **C23**, 2571 (1981)
[25] E Vigezzi and A Winther, *Ann. Phys.* **192**, 432 (1989)
[26] C V K Baba, V M Datar, K E G Löbner, A Navin and F J Schindler, *Phys. Lett.* **B338**, 147 (1994)
[27] G R Satchler, *Direct nuclear reactions* (Oxford University Press, New York, 1983)
[28] R A Broglia and A Winther, *Heavy ion reactions* (Addison-Wesley Publishing Company, Redwood City, CA, 1991) vol. 1